# Next-to-Leading-Order study on the associate production of $J/\psi + \gamma$ at the LHC

Rong Li[1,3] and Jian-Xiong Wang[2,3]
[1] *Department of Applied Physics, Xi'an Jiaotong University, Xi'an 710049, China.*
[2] *Institute of High Energy Physics, Chinese Academy of Sciences, P.O. Box 918(4), Beijing, 100049, China.*
[3] *Theoretical Physics Center for Science Facilities, CAS, Beijing, 100049, China.*
(Dated: January 28, 2014)

The associate $J/\psi+\gamma$ production at the LHC is studied completely at next-to-leading-order (NLO) within the framework of nonrelativistic QCD. By using three sets of color-octet long-distance matrix elements (LDMEs) obtained in previous prompt $J/\psi$ studies, we find that only one of them can result in a positive transverse momentum ($p_t$) distribution of $J/\psi$ production rate at large $p_t$ region. Based on reasonable consideration to cut down background, our estimation is measurable upto $p_t = 50$GeV with present data sample collected at 8TeV LHC. All the color-octet LDMEs in $J/\psi$ production could be fixed sensitively by including this proposed measurement and our calculation, and then confident conclusion on $J/\psi$ polarization puzzle could be achieved.

PACS numbers: 12.38.Bx, 13.25.Gv, 13.60.Le

arXiv:1401.6918v1 [hep-ph] 27 Jan 2014

Since the discovery of heavy quarkonium in the 1970s, the study on production and decay of $J/\psi$ and $\Upsilon$, plays an important role in the research on the perturbative and nonperturbative aspects of QCD. In 1995, a new factorization framework, nonrelativistic QCD (NRQCD), had been proposed to study the production and decay of heavy quarkonium [1]. It overcomes some shortcomings in the prevalent color-single model(CSM) [2] and makes the CSM be a part of it. By extracting the NRQCD long-distance matrix elements (LDMEs) from the matching between theoretical prediction and experimental data, the NRQCD calculation had given a well description on the transverse momentum distribution ($p_t$) of heavy quarkonium production at hadron colliders at leading order (LO) [3]. The phenomenological applications of the NRQCD have been investigated extensively [4]. But the polarization of heavy quarkonium hadroproduction had been an open question for more than ten years.

The next-to-leading order (NLO) QCD correction to the $J/\psi$ inclusive hadroproduction in the CSM significantly enhanced the $p_t$ distribution [5] and changed the polarization from transverse to longitudinal [6]. The later study including the contribution from color-octet model (COM) parts($^1S_0^8$ and $^3S_1^8$) at QCD NLO still can not give the satisfied prediction on the polarization of $J/\psi$ [7]. In Ref. [8], the study on P-wave charmonium hadroproduction with the feeddown from $\chi_{cJ}$ to $J/\psi$ had been obtained at QCD NLO. Soon after the $p_t$ distribution of $J/\psi$ production rate at full NLO QCD had been given by two groups [9, 10]. Then after two years, the $p_t$ distributions on polarization for direct $J/\psi$ hadroproduction at full NLO QCD were presented by two group [11, 12]. A few months later, a complete study [13] on the polarization of prompt $J/\psi$ hadroproduction with the feeddown contribution from $\chi_{cJ}$ included was given, and it present the first result at QCD NLO which can be compared with the experimental measurements directly since all the polarization measurements are for prompt $J/\psi$. The recent measurements at the LHC by CMS [14] and LHCb [15] show disagreement with the prediction [13]. However, the results from three groups [11–13] imply that the $\chi^2$ fit to extract the LDMEs of $J/\psi$ production is very sensitive to input condition due to the approximately linear correlation of the three color-octet contribution parts. Therefore, no solid conclusion on the polarization of $J/\psi$ could be achieved, and other relevant reliable perturbative prediction, which is experimental mensurable and can break the linear correlation in previous fit, is expected. Is the study on associate $J/\psi+\gamma$ hadroproduction at full QCD NLO a good candidate? Our study clearly indicates that it is a very good candidate with present data sample collected at 8TeV LHC.

In another way, for $\Upsilon$ hadroproduction, there are studies on the $p_t$ distribution of yield and polarization for the CS channel at QCD NLO [5, 6] and at the partial next-to-next-to-leading order [16]. The NLO QCD correction to $p_t$ distribution of the yield and polarization for $\Upsilon(1S, 3S)$ via S-wave CO states is presented in Ref. [17], and the NLO QCD correction to $p_t$ distribution of the yield for $\Upsilon(1S)$ via all the CO states is presented in Ref. [18]. The complete NLO study on polarization of prompt $\Upsilon$ hadroproduction has been achieved in Ref. [19], which can explain the recent measurement on the polarization of $\Upsilon(1S, 2S, 3S)$ at the LHC by CMS collaboration [20].

In addition to the study on important inclusive heavy quarkonium hadroproduction, study on the associate hadroproduction of heavy quarkonium and photon (or $W^{\pm}$,$Z^0$ bosons) was proposed as a supplemental channel to probe the gluon content in the proton [21] or to investigate the production mechanism of heavy quarkonium [22]. The NLO QCD correction to $J/\psi + W^{\pm}(Z^0)$ had been calculated in Ref. [23]. Our study [24] shows the NLO QCD correction to the associate $J/\psi+\gamma$ hadroproduction in the CSM enhanced the $p_t$ distribution largely in the high momentum region and changed the polarization from transverse to longitudinal. The relevant study [25] can reproduce our results in a partial NLO calculation. To obtain an experimental measurable observable at full QCD NLO, we present the study on associate $J/\psi + \gamma$ hadroproduction at the NLO with full

COM contribution in this work.

In the NRQCD framework the inclusive production of $J/\psi+\gamma$ can be factorized as

$$\sigma(p+\bar{p}\to J/\psi+\gamma+X)=\sum_{i,j}\int dx_1dx_2 \qquad (1)$$
$$\times\ G_p^i(x_1)G_{\bar{p}}^j(x_2)\hat{\sigma}(ij\to(Q\bar{Q})_n+\gamma+X)\langle O_n^{J/\psi}\rangle.$$

Here $G_{p(\bar{p})}^{i(j)}$ are the parton distribution functions(PDFs), $\hat{\sigma}$ presents the parton level cross section, and $\langle O_n^{J/\psi}\rangle$ are the LDMEs. The relevant parton level processes are listed as following

$$g+g\to Q\bar{Q}[^3S_1^1,{}^1S_0^8,{}^3S_1^8,{}^3P_J^8]+\gamma, \qquad (2)$$
$$g+g\to Q\bar{Q}[^3S_1^1,{}^1S_0^8,{}^3S_1^8,{}^3P_J^8]+\gamma+g, \qquad (3)$$
$$q+\bar{q}\to Q\bar{Q}[^3S_1^1,{}^1S_0^8,{}^3S_1^8,{}^3P_J^8]+\gamma, \qquad (4)$$
$$q+\bar{q}\to Q\bar{Q}[^1S_0^8,{}^3S_1^8,{}^3P_J^8]+\gamma+g, \qquad (5)$$
$$q(\bar{q})+g\to Q\bar{Q}[^3S_1^1,{}^1S_0^8,{}^3S_1^8,{}^3P_J^8]+\gamma+q(\bar{q}). \qquad (6)$$

In addition to the $p_t(J/\psi)$ distribution of the $J/\psi+\gamma$ hadroproduction at QCD NLO, the related polarization observable $\alpha$ of $J/\psi$ is also studied. $\alpha$ is measured by using the angular distribution of the decayed lepton pair in helicity frame and related to the spin density matrix of $J/\psi$ as

$$\alpha(p_t)=\frac{\mathrm{d}\sigma_{11}/\mathrm{d}p_t-\mathrm{d}\sigma_{00}/\mathrm{d}p_t}{\mathrm{d}\sigma_{11}/\mathrm{d}p_t+\mathrm{d}\sigma_{00}/\mathrm{d}p_t}. \qquad (7)$$

Here the "1" and "0" mean the transverse and longitudinal polarization of $J/\psi$ at the matrix element level. The calculations of spin density matrix for the $Q\bar{Q}[^3S_1^1,{}^3S_1^8,{}^1S_0^8]$ are as what have been done in other similar processes [7].

In handling the processes in the COM, there are two aspects which are different from the color-singlet case. The first is is that in process (6) $\gamma$ has chance to collinear with quark or anti-quark $q(\bar{q})$ in final states in some region of the phase space. This infrared divergence will cancel the infrared divergence in the QED correction of $pp\to J/\psi+g$. Because we observe the photon in the final states, it means that we have to impose a cut on this process to isolate a photon from the quark jet [26]

$$p_t^i\le p_t^\gamma\frac{1-\cos R_{\gamma_i}}{1-\cos\delta_0}\quad for\quad R_{\gamma_i}<\delta_0. \qquad (8)$$

The definitions of the $p_t^i$, $p_t^\gamma$, $\cos R_{\gamma_i}$ and the $\delta_0$ can be find in Ref. [26]. Here we set $\delta_0$ =0.7. For the consideration on the experimental measurement, we also set cut-off on the transverse momentum of the photon($p_t^\gamma$). Therefore the numerical results will rely heavily on this condition. The second is that the color-octet P-wave parts have additional infrared divergence which will be factorized into the LDMEs by using the same method as in Ref. [27]. In the calculation of real process $Q\bar{Q}[^3P_J^8]+\gamma+g$ hadroproduction, there is a soft divergence related to $Q\bar{Q}$ pair radiating the soft gluon and it can be factorized as an amplitude square of $Q\bar{Q}[^3S_1^8,\ ^3S_1^1]+\gamma$ hadroproduction times a soft factor which contain soft divergence. This divergence can be absorbed into the redefinition of the $Q\bar{Q}[^3S_1^8,\ ^3S_1^1]$ LDMEs at NLO and there are finite parts being left. Therefore, except the direct calculation of $Q\bar{Q}[^3P_J^8]$ state we also have to take into account the contribution from the left parts, which we call the q-term parts.

After generating the Fortran codes of these processes individually by using the Feynman Diagram Calculation (FDC) package [28] , we had checked the cancelation of infrared and ultraviolet divergence, the gauge invariance and the cut-independence respectively. Because of the complexity of the analytic expressions we use the quadruple precision program in some of the calculation to avoid the numerical instability.

To obtain the numerical results, we choose the following parameters and cut conditions. The charm quark mass $m_c$ is set as 1.5GeV and will vary from 1.4GeV to 1.6GeV to estimate the related uncertainty. The renormalization and factorization scales are set to $\mu_r=\mu_f=\mu_0=\sqrt{(2m_c)^2+p_t^2}$ and it will vary from $\mu_0/2$ to $2\mu_0$ to estimate the uncertainties. The NRQCD scale $\mu_\Lambda$ is chosen as $m_c$. As for the experimental conditions, we use $\sqrt{s}=7,8,14$TeV at the LHC, the rapidity cuts $|y_{J/\psi,\gamma}|\le 3$, or pseudo-rapidity cut $|\eta_\gamma|\le 1.45$ and $p_t^\gamma<1.5,3,5,15$GeV cuts. The fine structure constant is chosen as $\frac{1}{128}$. The CTEQ6L1 and the CTEQ6M PDFs and the corresponding $\alpha_s$ running formula are used to calculate the LO and the NLO numerical results [29].

The involved LDMEs were extracted at the NLO by different group with different consideration [10, 12, 13, 30]. In Ref. [31] the authors investigated these LDME sets and concluded that the universality of LDMEs is challenged. The two LDME sets in Ref. [10, 12] are from the same group, and we use their former results on the combination of LDMEs in Ref. [10] to estimate numerical results since the feeddown contribution from $\chi_c$ and $\psi'$ had been considered there, which could affect the theoretical prediction largely as discussed in Ref. [13]. We list these LDME sets in table I. For the LDMEs in Reference [10], only the combinations of them, $M_{0,r_0}^{J/\psi}$ and $M_{1,r_1}^{J/\psi}$, are given as

$$M_{0,r_0}^{J/\psi}=\langle O^{J/\psi}(^1S_0^8)\rangle+\frac{r_0}{m_c^2}\langle O^{J/\psi}(^3P_0^8)\rangle, \qquad (9)$$
$$M_{1,r_1}^{J/\psi}=\langle O^{J/\psi}(^3S_1^8)\rangle+\frac{r_1}{m_c^2}\langle O^{J/\psi}(^3P_0^8)\rangle, \qquad (10)$$

where $r_0$=3.9, $r_1$=-0.56, $M_{0,r_0}^{J/\psi}=0.074$ and $M_{1,r_1}^{J/\psi}=0.0005$. With requiring the LDMEs to be positive we set the three individual color-octet LDMEs from the above combinations under two conditions in table I, which we will refer to as "Ma extension" in the following parts.

It is shown in Fig.1 that the color-octet $^3P_J^8$ state, just like $^3S_1^8$ and $^1S_0^8$ state, gives a positive short distance coefficient in all $p_t$ region in contrast to $J/\psi$ inclusive

TABLE I: The NRQCD LDMEs $\langle O^{J/\psi}(n)\rangle$ extracted by three groups in Ref. [10, 12, 13, 30] at the NLO with $\langle O^{J/\psi}(^3S_1^1)\rangle$ =1.32 (1.16) GeV$^3$ used in Ref. [30] (in the others). The NRQCD LDMEs in Ma extension1 and extension2 are determined from the combination extracted in Ref. [10].

| $n$ | $^1S_0^8$, GeV$^3$ | $^3S_1^8$, GeV$^3$ | $^3P_0^8$, GeV$^5$ |
|---|---|---|---|
| Butenschoen[30] | 0.0497 | 0.0022 | −0.0161 |
| Gong[13] | 0.097 | −0.0046 | −0.0214 |
| Chao[12] | 0.089 | 0.0030 | 0.0126 |
| Ma extension1 | 0.074 | 0.0005 | 0 |
| Ma extension2 | 0 | 0.011 | 0.019 |

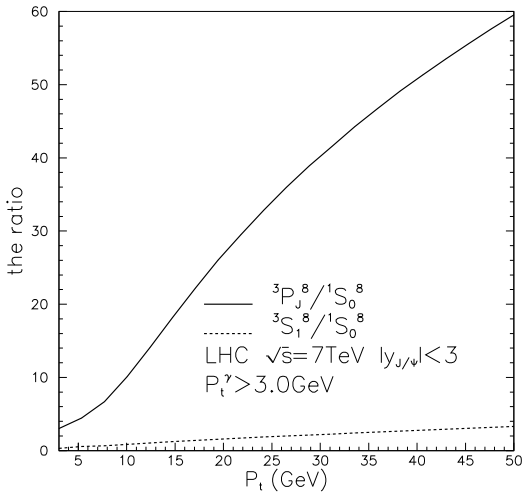


FIG. 1: The ratio of $d\sigma(^3P_J^8)/d\sigma(^1S_0^8)$ and $d\sigma(^3S_1^8)/d\sigma(^1S_0^8)$ as functions of $p_t$.

hadroproduction at QCD NLO case where the color-octet $^3P_J^8$ state gives negative short distance coefficient in large $p_t$ region. The difference makes the $p_t$ distribution of $J/\psi+\gamma$ production rate an observable which can break the linear correlation in previous fit.

The first column of Fig.2 presents the results at $\sqrt{s}=$ 7TeV. In order to investigate the dependence on $p_t^\gamma$ cut, we plot the $p_t$ distribution of production rate and polarization observable $\alpha$ with different $p_t^\gamma$ cuts and two sets of the LDMEs in Ma extension. The plots show that the dependence on $p_t^\gamma$ cut decreases with the increase of $p_t(J/\psi)$ and different $p_t^\gamma$ cuts make the $p_t$ distribution shift parallel in contrast to the color-singlet channel in Ref. [24] where the $p_t$ distribution of $J/\psi$ production rate and $\alpha$ are insensitive to the the $p_t^\gamma$ cut in the same $p_t$ region. The reason is that $^3P_J^8$ and $^1S_0^8$ channel in the COM are sensitive to the cuts.

In the second column in Fig.2, we give results at $\sqrt{s}=14$TeV. The shaded band represents the uncertainties estimated by varying the $m_c$, the renormalization scale $\mu_r$ and factorization scale $\mu_f$. The plots show that the uncertainties of production rate become larger and that of $\alpha$ become smaller as $p_t$ increasing. The COM contribution on production rate dominant over that of CSM and are about 2 orders larger than the color-singlet ones at $p_t=50$GeV. We also plot the $p_t$ distribution with the LDME sets in Ref. [30] and [13], the absolute value of the numerical results are used in the $p_t$ distribution of production rate since they become negative when $p_t>13$GeV, and $\alpha$s in both cases are out of physical region when $p_t>10GeV$.

From the results at the first and second columns of Fig.2, we know that the $p_t$ distribution of $J/\psi+\gamma$ hadroproduction rate is good observable to distinguish different LDME sets. Is it measurable or not at the 8GeV LHC with present 23fb$^{-1}$ integrated luminosity? To suppress the background efficiently, $p_t^\gamma>15$GeV cut on photon is applied, together with $|y_{J/\psi}|<2.4$ and $|\eta_\gamma|<1.45$ for photon reconstruction efficiency consideration. The plots in the third column of Fig.2 show that the $p_t$ distributions of $J/\psi$ production rate in the COM with Ma extension LDME sets are about 10(100) times larger than that in the CSM. The other two LDME sets give the positive predictions in lower $p_t$ region and negative ones when $p_t$ is larger than 31 GeV. When $p_t$ is larger than 20GeV, the results show many differences on the $J/\psi$ polarization predictions $\alpha$ with the CSM (COM) mechanism and three LDME sets. It is mentionable that only real processes at QCD NLO contribute when $p_t^{J/\psi}<15$GeV.

In summary, we present the study on associate $J/\psi+\gamma$ hadroproduction at the NLO with full COM contribution at the LHC. Our numerical results show that the contribution from color-octet channels enhances the differential cross section about 2 order in the large $p_t$ region. As for the $J/\psi$ polarization, the color-octet contribution changes it from longitudinal one to transverse one. From all the plots in Fig.2, it is manifestly that the most important uncertainty comes from the the variation of LDMEs. The LDME sets of Butenschoen and Gong lead to the unphysical $p_t$ distribution of production rate (negative) and polarization observable $\alpha$ (out of range -1 to 1) at large $p_t$ range, while the LDME set of Ma extension gives physical ones at all the $p_t$ range. Even within Ma extension, the $p_t$ distributions of production rate are of huge difference ( 10 times at $p_t=50$GeV) between the extension2 and extension1. The polarization observable $\alpha$ changes from slightly longitudinal in extension1 to the transverse in extension2.

In conclusion, the theoretical predictions are sensitive to the LDMEs heavily and can break the linear correlation in previous fit. To obtain an experimental measurable observable at the 8GeV LHC with present 23fb$^{-1}$ integrated luminosity, $p_t^\gamma>15$GeV cut on the observed photon is applied to efficiently suppress the background and $|\eta_\gamma|<1.45$ is used. With these conditions, the photon reconstruction efficiency is larger than 0.7 and we use 0.7

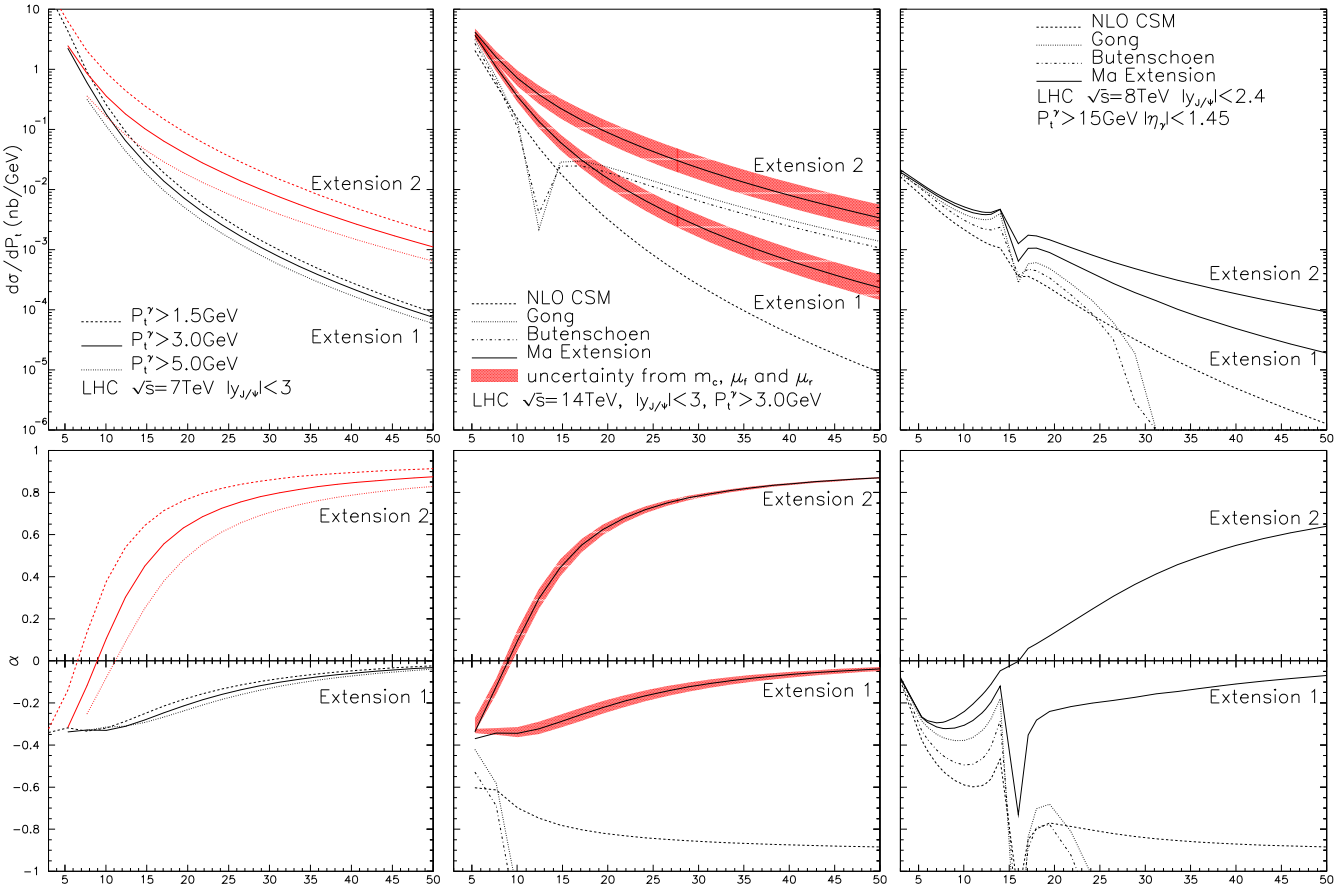


FIG. 2: The $p_t(J/\psi)$ distributions for $J/\psi+\gamma$ production (upper parts) and polarization (lower parts) with different conditions. Figures in the same column are of the same conditions and line types. The shaded band in the second column represent the uncertainty from variation of $\mu_f$ & $\mu_r$ and $m_c$. The third column shows results with $p_t^\gamma > 15$GeV and different LDME sets.

in the following estimation, $Br(J/\psi \to \mu^+ + \mu^-) = 0.05$ is also used to represent reconstruction of $J/\psi$ from the observed $\mu^+ + \mu^-$ pair. Then the plots in the third column of Fig.2 indicates that 800-1600 events at $p_t = 17$Gev and 16-80 events at $p_t = 50$GeV could be reconstructed from the sample data. Therefore, the $p_t$ distribution of production rate is experimental measurable with present data sample collected at 8TeV LHC. All the color-octet LDMEs in $J/\psi$ production could be fixed sensitively by including this proposed measurement and our calculation.

We thank Dr. Bin Gong, Hong-Fei zhang and Lu-Ping Wan for helpful discussions. Rong Li also thanks Qiang Li for the discussion on the isolation of photon. This work is supported by the National Natural Science Foundation of China (No. 11105152, 10935012, and No. 11005137), DFG and NSFC (CRC110), and by CAS under Project No. INFO-115-B01.

[1] G. T. Bodwin, E. Braaten and G. P. Lepage, Phys. Rev. D **51**, 1125 (1995) [Erratum-ibid. D **55**, 5853 (1997)].
[2] M. B. Einhorn and S. D. Ellis, Phys. Rev. D **12**, 2007 (1975); S. D. Ellis, M. B. Einhorn and C. Quigg, Phys. Rev. Lett. **36**, 1263 (1976); C. -H. Chang, Nucl. Phys. B **172**, 425 (1980); E. L. Berger and D. L. Jones, Phys. Rev. D **23**, 1521 (1981); R. Baier and R. Ruckl, Nucl. Phys. B **201**, 1 (1982).
[3] P. L. Cho and A. K. Leibovich, Phys. Rev. D **53**, 150 (1996); Phys. Rev. D **53**, 6203 (1996).
[4] N. Brambilla *et al.* [Quarkonium Working Group Collaboration], hep-ph/0412158; J. P. Lansberg, Int. J. Mod. Phys. A **21**, 3857 (2006).
[5] J. M. Campbell, F. Maltoni and F. Tramontano, Phys. Rev. Lett. **98**, 252002 (2007).
[6] B. Gong and J. -X. Wang, Phys. Rev. Lett. **100**, 232001 (2008); Phys. Rev. D **78**, 074011 (2008).
[7] B. Gong, X. Q. Li and J. -X. Wang, Phys. Lett. B **673**, 197 (2009) [Erratum-ibid. **693**, 612 (2010)].
[8] Y. -Q. Ma, K. Wang and K. -T. Chao, Phys. Rev. D **83**, 111503 (2011).
[9] M. Butenschoen and B. A. Kniehl, Phys. Rev. Lett. **106**,

022003 (2011).
[10] Y. -Q. Ma, K. Wang and K. -T. Chao, Phys. Rev. Lett. **106**, 042002 (2011).
[11] M. Butenschoen and B. A. Kniehl, Phys. Rev. Lett. **108**, 172002 (2012).
[12] K. -T. Chao, Y. -Q. Ma, H. -S. Shao, K. Wang and Y. -J. Zhang, Phys. Rev. Lett. **108**, 242004 (2012).
[13] B. Gong, L. -P. Wan, J. -X. Wang and H. -F. Zhang, Phys. Rev. Lett. **110**, 042002 (2013).
[14] S. Chatrchyan *et al.* [CMS Collaboration], Phys. Lett. B **727**, 381 (2013) [arXiv:1307.6070 [hep-ex]].
[15] RAaij *et al.* [LHCb Collaboration], Eur. Phys. J. C **73**, 2631 (2013) [arXiv:1307.6379 [hep-ex]].
[16] P. Artoisenet, J. M. Campbell, J. P. Lansberg, F. Maltoni, and F. Tramontano, Phys. Rev. Lett. **101**, 152001 (2008).
[17] B. Gong, J.-X. Wang, and H.-F. Zhang, Phys. Rev. D **83**, 114021 (2011).
[18] K. Wang, Y.-Q. Ma and K.-T. Chao, Phys. Rev. D **85**, 114003 (2012).
[19] B. Gong, L. -P. Wan, J. -X. Wang and H. -F. Zhang, Phys. Rev. Lett. **112**, 032001 (2014).
[20] S. Chatrchyan *et al.* [CMS Collaboration], Phys. Rev. Lett. **110**, 081802 (2013).
[21] M. Drees and C. S. Kim, Z. Phys. C **53**, 673 (1992); M. A. Doncheski and C. S. Kim, Phys. Rev. D **49**, 4463 (1994).
[22] C. S. Kim and E. Mirkes, Phys. Rev. D **51**, 3340 (1995); E. Mirkes and C. S. Kim, Phys. Lett. B **346**, 124 (1995); D. P. Roy and K. Sridhar, Phys. Lett. B **341**, 413 (1995); C. S. Kim, J. Lee and H. S. Song, Phys. Rev. D **55**, 5429 (1997); P. Mathews, K. Sridhar and R. Basu, Phys. Rev. D **60**, 014009 (1999); B. A. Kniehl, C. P. Palisoc and L. Zwirner, Phys. Rev. D **66**, 114002 (2002); J. P. Lansberg and C. Lorce, Phys. Lett. B **726**, 218 (2013).
[23] G. Li, M. Song, R. -Y. Zhang and W. -G. Ma, Phys. Rev. D **83**, 014001 (2011); S. Mao, M. Wen-Gan, L. Gang, Z. Ren-You and G. Lei, JHEP **1102**, 071 (2011) [Erratum-ibid. **1212**, 010 (2012)]; B. Gong, J. -P. Lansberg, C. Lorce and J. Wang, JHEP **1303**, 115 (2013).
[24] R. Li and J. -X. Wang, Phys. Lett. B **672**, 51 (2009).
[25] J. P. Lansberg, Phys. Lett. B **679**, 340 (2009).
[26] S. Frixione, Phys. Lett. B **429**, 369 (1998).
[27] J. -X. Wang and H. -F. Zhang, Phys. Rev. D **86**, 074012 (2012).
[28] J. -X. Wang, Nucl. Instrum. Meth. A **534**, 241 (2004).
[29] J. Pumplin, D. R. Stump, J. Huston, H. L. Lai, P. M. Nadolsky and W. K. Tung, JHEP **0207**, 012 (2002).
[30] M. Butenschoen and B. A. Kniehl, Phys. Rev. D **84**, 051501 (2011).
[31] M. Butenschoen and B. A. Kniehl, Mod. Phys. Lett. A **28**, no. 9, 1350027 (2013).

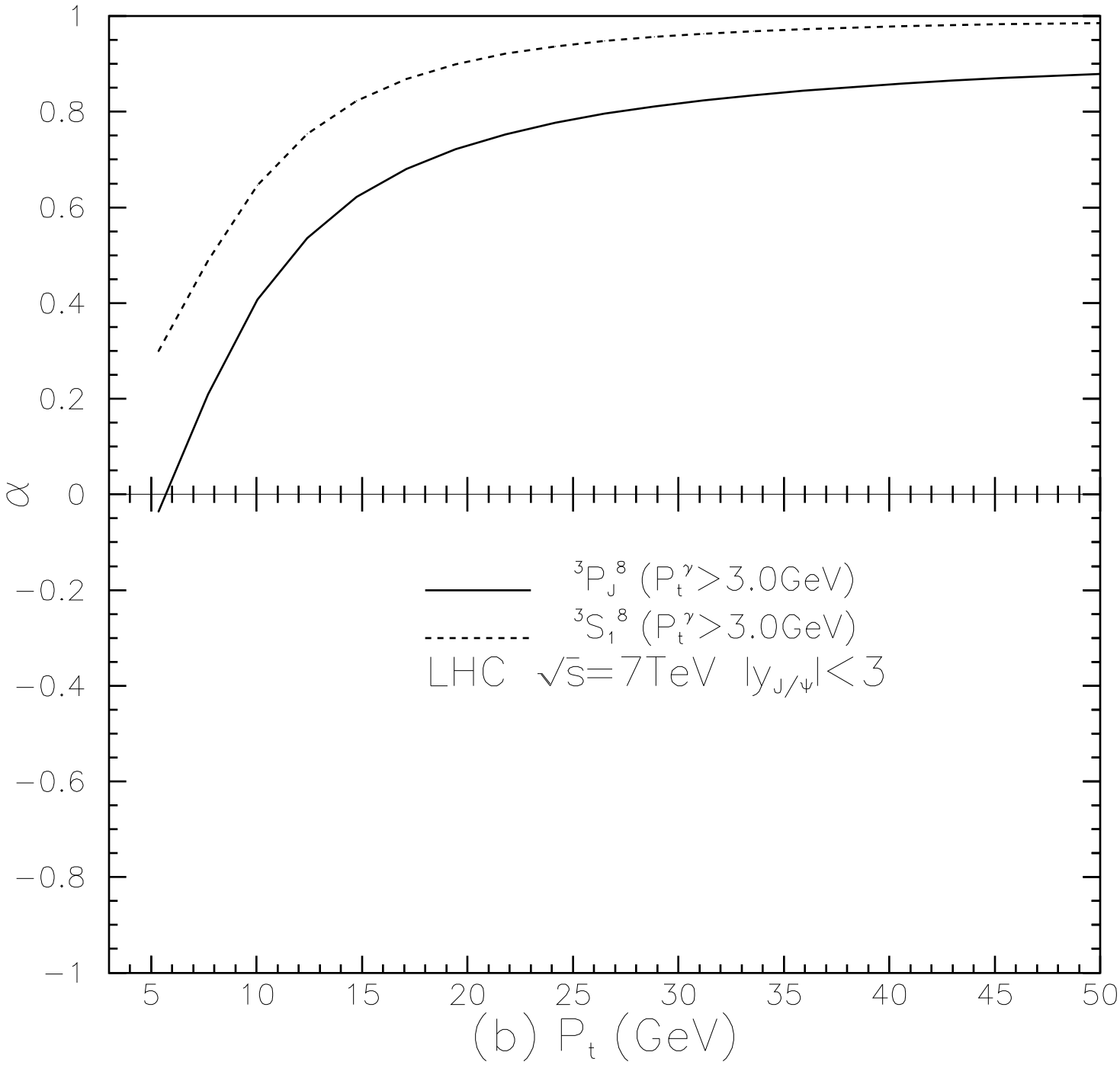
1
0.8
0.6
0.4
0.2
0
−0.2
−0.4
−0.6
−0.8
−1
α
5
10
15
20
25
30
35
40
45
50
(b) $P_t$ (GeV)
$^3P_J^8$ ($P_t^\gamma$>3.0GeV)
$^3S_1^8$ ($P_t^\gamma$>3.0GeV)
LHC $\sqrt{s}$=7TeV $|y_{J/\psi}|$<3